

Nanoparticle-Terpene Fusion: A Game-Changer in Combating Primary Amoebic Meningoencephalitis Caused by *Naegleria fowleri*

Kavitha Rajendran,* Usman Ahmed, Alexia Chloe Meunier, Mohd Farooq Shaikh, Ruqaiyyah Siddiqui, and Ayaz Anwar*



Cite This: *ACS Omega* 2024, 9, 11597–11607



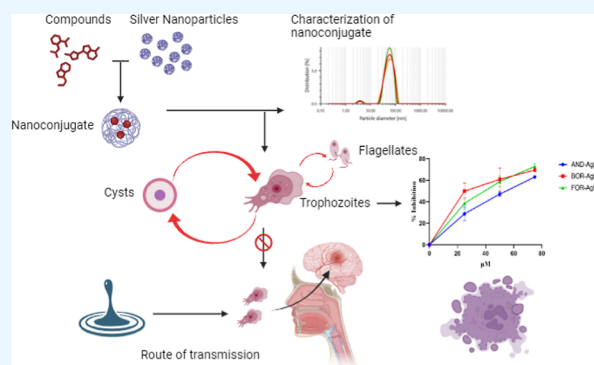
Read Online

ACCESS |

Metrics & More

Article Recommendations

ABSTRACT: Pathogenic *Naegleria fowleri* (*N. fowleri*) are opportunistic free-living amoebae and are the causative agents of a very rare but severe brain infection called primary amoebic meningoencephalitis (PAM). The fatality rate of PAM in reported cases is more than 95%. Most of the drugs used against *N. fowleri* infections are repurposed drugs. Therefore, a large number of compounds have been tested against *N. fowleri* in vitro, but most of the tested compounds showed high toxicity and an inability to cross the blood–brain barrier. Andrographolide, forskolin, and borneol are important natural compounds that have shown various valuable biological properties. In the present study, the nanoconjugates (AND-AgNPs, BOR-AgNPs, and FOR-AgNPs) of these compounds were synthesized and assessed against both stages (trophozoite and cyst) of *N. fowleri* for their antiamoebic and cysticidal potential in vitro. In addition, cytotoxicity and host cell pathogenicity were also evaluated in vitro. FOR-AgNPs were the most potent nanoconjugate and showed potent antiamoebic activity against *N. fowleri* with an IC_{50} of 26.35 μ M. Nanoconjugates FOR-AgNPs, BOR-AgNPs, and AND-AgNPs also significantly inhibit the viability of *N. fowleri* cysts. Cytotoxicity assessment showed that these nanoconjugates caused minimum damage to human keratinocyte cells (HaCaT cells) at 100 μ g/mL, while also effectively reducing the cytopathogenicity of *N. fowleri* trophozoites to the HaCaT cells. The outcomes of our experiments have unveiled substantial potential for AND-AgNPs, BOR-AgNPs, and FOR-AgNPs in the realm of developing innovative alternative therapeutic agents to combat infections caused by *N. fowleri*. This study represents a significant step forward in the pursuit of advanced strategies for managing such amoebic infections, laying the foundation for the development of novel and more effective therapeutic modalities in the fight against free-living amoebae.



INTRODUCTION

Naegleria fowleri known as a “brain-eating” amoeba is a thermostable free-living protist widely distributed in the environment.¹ They are most commonly found in fresh water and moist soil, the amoeba proliferates in hot summer conditions as they can withstand temperatures of up to 45 °C.² *N. fowleri* usually feeds on bacteria found in naturally occurring warm freshwater bodies, where it has been commonly found.^{2,3} Based on various environmental conditions, the amphibolic amoeba exists in three distinct phenotypic phases; trophozoite, flagellate, and cyst. Under favorable conditions, *Naegleria* exists in the metabolically active trophozoite stage ranging in size from 10 to 25 μ m. In this stage, it can be divided by binary fission and cause infection.^{1,2,4} When resources are depleted in watery conditions, the trophozoites transform into a pear-shaped flagellate phase, ranging in size from 10 to 16 μ m.^{1,2} It allows *N. fowleri* to move a long distance in the presence of a nutritious environment. However, in adverse conditions (high

salinity, temperature, and low pH), the amoeba transforms into a cyst stage, ranging in size from 8 to 20 μ m.⁵

N. fowleri is the only human pathogenic species in the genus and is the causative agent of a serious, fatal disease known as primary amoebic meningoencephalitis (PAM). More than 90% of the cases showed that *Naegleria* infects the central nervous system (CNS) of adults and children.⁶ While swimming in contaminated water, pool, and unchlorinated swimming pool, the pathogen enters the body through the nasal cavity.⁷ It then penetrates the olfactory neuroepithelium to the central nervous system, causing a deadly infection. In most cases, the infection is clinically misdiagnosed as acute bacterial meningitis due to

Received: November 7, 2023

Revised: December 17, 2023

Accepted: December 22, 2023

Published: March 1, 2024



similar symptoms and limited information about the pathogen.⁸ Initial signs and symptoms of the infection are severe headache, fever, stiff neck, and convulsions.⁹ Chemotherapy is the most common method for the treatment of *N. fowleri* infection. The current therapy includes combinations of different drugs. To date, no clinical trial has been performed due to the rarity of PAM infection. The efficacy of drugs is based on case reports of the infection. Amphotericin B (AmpB), a polyene antifungal medication, is the preferred drug for treating PAM. Other drugs used for treating PAM are miltefosine, rifampin, azithromycin, and different azoles.¹⁰

However, most of these drugs are ineffective against the cyst stage of *Naegleria*, and the presence of cysts in the brain may result in the recurrence of the infection.¹¹ These drugs also showed severe side effects including high toxicity to body cells.¹² Some drugs are still undergoing research and their absolute bioavailability is unknown.¹³ Most of the drugs are unable to cross the blood–brain barrier (BBB) and hence are ineffective *in vivo*. To overcome these limitations, there is an urgent need for the development of new alternative safe drugs that have efficacy to target both trophozoite and cyst forms of *N. fowleri*.

PAM infection can be treated effectively using nanomedicine. Nanoparticles with therapeutic activities have evolved in the field of precision medicine.¹⁴ The conjugation has shown various benefits for treating a variety of diseases.¹⁵ They have increased drug delivery, pharmacokinetics, bioavailability, and decreased toxicity.¹⁶ The nanoparticles conjugated with compounds showed potent antibacterial, antiamoebic, and antiviral activities.^{16,17} Similarly, the silver nanoparticles (AgNPs) conjugated with different clinically approved drugs such as AmpB have been used against *N. fowleri* and have shown enhanced activity as compared to drugs alone.¹⁸ Nanoparticles coated with natural compounds (cinnamic acid, betulinic acid, and tannic acid) and plant extract have been effectively used against *Acanthamoeba castellanii*.^{19–22} Silver nanoconjugates showed the most potent antiamoebic effect as compared to other nanoconjugates.²² Based on these studies, we coated AgNPs with natural compounds and tested them against *N. fowleri* *in vitro*. Therefore, previously we tested a library of natural compounds against *N. fowleri*, and we found that some compounds showed potent activity.

Andrographolide (AND) is a natural compound that is extracted from *Andrographis paniculate* and has shown a wide range of biological activities such as anti-inflammatory, antibacterial, antiviral, etc. It has shown higher bioavailability with a thoroughly investigated mode of action.²³ Borneol (BOR), which is usually used as a medicine in China and India, has a wide spectrum of biological activities. The compound has shown anti-inflammatory, antibacterial, neuroprotective, increased BBB permeability etc. The compound is also effective for nanodrug delivery.²⁴ Forskolin (FOR) is a diterpene and is extracted from the herb *Coleus forskohlii*.²⁵ The compound also showed a wide range of biological and pharmaceutical effects. The root of the plant is used as a folk medicine and for the treatment of hypertension, respiratory disorders, and eczema, and it has shown potent activity against *Entamoeba histolytica*.^{26,27}

Therefore, we hypothesized that selected natural compounds (thymol, BOR, FOR, and AND) will be conjugated with AgNPs and will be assessed against both trophozoite and cyst stage of *N. fowleri*. AgNPs were successfully coated and showed potent activity *in vitro* as compared to the vehicle control and

showed limited toxicity to HaCaT cells. We speculate that selected nanoconjugates might make it possible to discover a new potential therapeutic agent that is effective against PAM infection.

MATERIALS AND METHODS

Consumables. All of the materials employed in this study were of analytical quality. The medium, such as Roswell Park Memorial Institute 1640 medium (RPMI-1640) and phosphate-buffered saline, and their supplements, such as minimum essential medium nonessential amino acids (MEM-NEAA) and L-glutamine, were procured from Nacalai Tesque, based in Kyoto, Japan. Other chemicals, such as dimethyl sulfoxide (DMSO) and silver nitrate (AgNO₃), were procured from Thermo Fisher Scientific, based in Massachusetts, USA. Triton X-100 and trypan blue were acquired from Sigma-Aldrich, located in Saint Louis, USA. Additionally, miltefosine was acquired from Sigma-Aldrich, located in San Francisco, USA.

HaCaT and HeLa Cell Lines. HeLa cells are a widely used human cell line derived from cervical cancer patient and are required for *N. fowleri* culture, while HaCaT cells are a widely used human keratinocyte cell line required for cytotoxicity. Both frozen cell line vials were retrieved from liquid nitrogen storage and swiftly thawed in a 37 °C water bath until only a small ice crystal remained. The cells were centrifuged (1500 rpm) in a prewarmed supplemented RPMI-1640 [10% FBS, 1% pen-strep, L-glutamine (2 mM), and nonessential amino acid]. The supernatant was carefully aspirated, and the cell suspension was transferred to a 75 cm² flask. Finally, the cell culture vessels were placed in a 37 °C, 5% CO₂ incubator. The flasks were monitored under a microscope until a monolayer was observed. The monolayer was trypsinized, and the cell suspension was seeded in multiwell plates for further assessments. The cells were also regularly checked for mycoplasma contamination.^{28,29}

***N. fowleri* Culture and Maintenance.** In the current investigation, the *N. fowleri* strain used was obtained from a clinical isolation originating from a patient's cerebrospinal fluid. This strain was procured from the American type culture collection (ATCC) 30,174 repository. The trophozoites were revived, cultured, subcultured, and maintained in RPMI-1640 supplemented with antibiotics, such as penicillin, streptomycin, and gentamycin. The trophozoites were thawed and centrifuged at 2500 rpm in 10 mL of supplemented RPMI-1640. The 10 mL suspension of *N. fowleri* trophozoites were inoculated to the monolayer of HeLa cell line in a 75 cm² tissue culture flask. The plates with the *N. fowleri* trophozoites and RPMI-1640 medium were placed in a CO₂ incubator set at 37 °C. Regularly, the growth of trophozoites was checked until the monolayer was completely finished. The cells were subcultured or used for an experiment by transferring a portion of the trophozoites into a fresh supplemented RPMI-1640 medium. RPMI-1640 medium was employed to sustain both the population and morphological characteristics of *N. fowleri* cells within all experimental groups under examination.²⁸

***N. fowleri* Cyst Formation.** The cyst formation was induced by transferring the actively growing *N. fowleri* trophozoites to an empty 75 cm² tissue culture flask. The flasks were maintained at a temperature lower than 37 °C. Lowering the temperature and depletion of nutrients (maintaining cells only in RPMI-1640) mimic stressful conditions and trigger cyst formation. The culture was observed regularly under the microscope until circular or

oval double-walled cysts were observed.²⁸ The cysts were stored at 4 °C for future use.

Synthesis of the Natural Compound-Coated AgNPs.

The natural compound-coated AgNPs were synthesized through a chemical process. In this method, an aqueous solution of AgNO₃ was combined with sodium borohydride, serving as a reducing agent. This reaction took place in the presence of an aqueous solution of three natural compounds: AND, BOR, and FOR, each at a concentration of 1 μM. The procedure involves mixing equal volumes of compounds with 1 μM AgNO₃ in sample bottles. Subsequently, 5 mM sodium borohydride was added drop by drop, and the mixture was stirred for 2 h. During this time, the color of the mixture transitioned from light yellow to dark brown, indicating the reduction of silver ions by sodium borohydride. This served as a visual indicator of the nanoconjugate synthesis. Following this, the colloidal suspension underwent further characterization to confirm the successful synthesis of the nanoconjugates.³⁰

Characterization. The freshly synthesized andrographolide-AgNPs (AND-AgNPs), borneol-AgNPs (BOR-AgNPs), and forskolin-AgNPs (FOR-AgNPs) were subjected to characterization through various techniques, including ultraviolet–visible (UV–vis) spectrophotometry (performed with a Thermo Fischer, Evolution 210), transmission electron microscopy (TEM), particle analysis, and zeta potential analysis.³⁰

Antiamoebic Assessment. This assay involves testing the efficacy of various treatments (nanoconjugates) against the protozoan parasite *N. fowleri*, which can cause serious central nervous system infections. The assay was performed as conducted by Ahmed et al.²⁸ and Rajendran et al.³¹ Briefly, the trophozoites were harvested, and a standard number of cells (3 × 10⁵ cells/mL) were added to the wells of a microtiter plate. The tested nanoconjugates (AND-AgNPs, BOR-AgNPs, and FOR-AgNPs) were diluted at the desired concentrations (25, 50, and 75 μM) and added to separate wells. Specific wells were specified for positive (100 μM miltefosine), negative, solvent (water and DMSO), and vehicle (AgNPs) controls. The plates containing the treated trophozoites were incubated at 37 °C for 24 h. The assay was performed in RPMI-1640 to maintain the number of trophozoites in each well.

Cysticidal Assessment. The cysts were harvested and a cysticidal assay was performed according to the previously described procedure.^{28,31} Specifically, the 1 × 10⁵ cyst/mL were counted, and they were subsequently placed in a multiwell plate for experimentation. The cysts were exposed to various concentrations (25, 50, and 75 μM) of the tested nanoconjugates (AND-AgNPs, BOR-AgNPs, and FOR-AgNPs) in the RPMI-1640 medium to determine the dose–response relationship. As a negative control, cysts were cultured in RPMI-1640 alone, while water and DMSO served as the solvent control. Miltefosine was employed as the positive control in this study. The cysts were placed in a 5% CO₂ incubator at 37 °C and allowed to incubate for a duration of 72 h.

Evaluation. After incubation, the antiamoebic and cysticidal activity of nanoconjugates were evaluated by trypan blue exclusion test. The treated and control wells were examined under an inverted microscope to observe viability, morphology, and growth inhibition. The viable trophozoites (unstained) were counted in each well by a hemocytometer. The growth inhibition and the IC₅₀ (concentration at which

50% of amoebae are inhibited) for each compound were calculated.²⁸

Cell Cytotoxicity Assays. A lactate dehydrogenase (LDH) detection kit is a common method used to assess the cytotoxic effects of nanoconjugates on the HaCaT cell line. The HaCaT cells were maintained in an appropriate culture medium (as stated in the upper section) under standard cell culture conditions, i.e., 37 °C, 5% CO₂. The cells were harvested and placed in a 96-well plate. The cells were placed in a 5% CO₂ incubator at 37 °C and allowed to incubate for 24 h. After incubation, the monolayer was treated with different concentrations (25, 50, and 75 μM) of AND-AgNPs, BOR-AgNPs, and FOR-AgNPs. Appropriate wells (untreated cells) were selected as a negative control, while monolayers treated with Triton X-100 served as the positive control.^{30,32,33}

LDH Assay. After incubation period, the plates were centrifuged, and 25 μL of supernatant was collected from each well, which contained the released LDH from dead or damaged cells. A replica of a microtiter plate was made, and LDH detection kit (Invitrogen, Illinois, USA) ingredients were added to each well as manufacturer's recommendations. The plates were incubated for 10 min. The microplate reader was used to record the absorbance at 490 nm.³³ The percentage (%) of cytotoxicity was calculated using the formula

$$\text{cytotoxicity \%} = \frac{\text{release} - \text{untreated LDH release}}{(\text{Triton X} - 100 \text{ LDH release} - \text{untreated LDH release})} \times 100$$

Cytopathogenicity. The cytopathogenicity assay was performed against the HaCaT cell line as stated earlier.³⁴ The assay was performed using an LDH kit following the manufacturer's instructions provided with the LDH detection kit (Invitrogen, Illinois, USA). Briefly, the antiamoebic assay was performed by treating 5 × 10⁵ *N. fowleri* trophozoites with different concentrations (25, 50, and 75 μM) of AND-AgNPs, BOR-AgNPs, and FOR-AgNPs for 2 h. The pretreated trophozoites were collected and resuspended in RPMI-1640. The monolayer of HaCaT cells was treated with pretreated trophozoites in duplicate wells, including control wells with untreated cells and some specified for Triton X-100 treatment. Incubate the cells with the trophozoites for 24 h at 37 °C and 5% CO₂. After the incubation, an LDH assay was performed. The measurement of absorbance was taken at a wavelength of 490 nm, and the percentage of cytopathogenicity was determined using the cytotoxicity formula (given above).

RESULTS

Characterization of the AgNPs Coated with Natural Compounds. AgNPs coated with natural compounds were successfully synthesized by the reduction of AgNO₃ in an aqueous solution of thymol, AND, BOR, and FOR, as meticulously outlined in the **Materials and Methods** section. It is noteworthy, however, that the nanoconjugates involving thymol (THY-AgNPs) exhibited an unprecedented degree of instability, rendering them unsuitable for further characterization and in vitro assessment of biological activities.

The synthesis of AND-AgNPs, BOR-AgNPs, and FOR-AgNPs was confirmed by using UV–visible spectrophotometry at a range of 200–600 nm. The AND-AgNPs, BOR-AgNPs, and FOR-AgNPs gave distinct surface plasmon resonance

bands at 441, 410, and 415 nm, respectively. These are typical examples of stable, medium-sized AgNPs, confirming that nanoconjugates were successfully synthesized.

The surface morphology of nanoconjugates was analyzed by TEM. The TEM micrograph analysis of AND-AgNPs, BOR-AgNPs, and FOR-AgNPs showed that all nanoconjugates were regular and rounded in shape (Figure 1A–C).

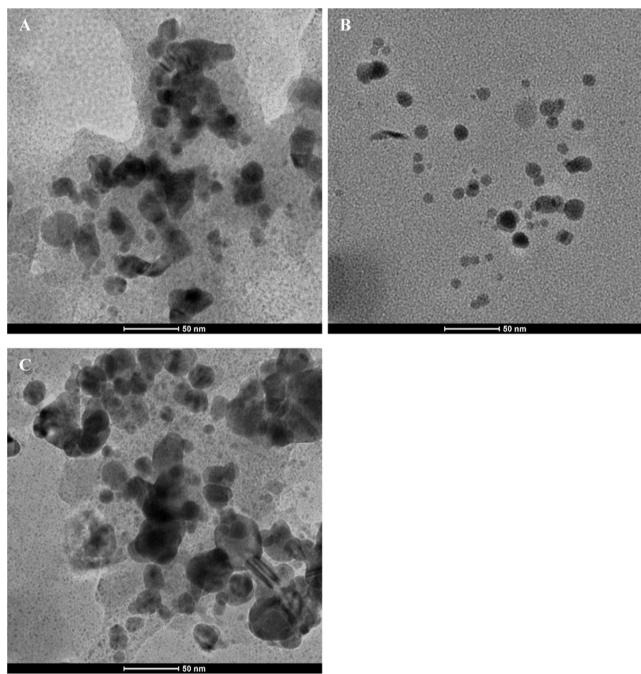


Figure 1. TEM micrographs were captured to reveal the structural characteristics of biologically synthesized nanoconjugates. The images, depicted at a 50 nm scale bar, present distinct nanoconjugates formed from (A) AND-AgNPs, (B) BOR-AgNPs, and (C) FOR-AgNPs. These microscopic analyses offer insights into the morphology and size distribution of the newly synthesized nanoconjugates.

Two parameters—size and shape—play a key role in designing a drug delivery system against infection. The smaller the size, the greater the surface-to-volume ratio and vice versa. The smaller size offers a higher chance of coating nanoparticles with therapeutic agents, thereby increasing the efficacy and bioavailability of the drug.³⁵ The particle analyzer showed that the average sizes of AND-AgNPs, BOR-AgNPs, and FOR-AgNPs were 52.73, 52.34, and 80.33 nm (Figure 2A–C).

Another important parameter used for the determination of the nanoconjugate stability is the zeta potential. Figure 3A–C shows that all nanoconjugates were anionic in nature. The surface charge distribution values of AND-AgNPs, BOR-AgNPs, and FOR-AgNPs were -131.1 , -105.9 , and -122.1 mV, respectively. No change in color or precipitation was evident for more than 6 months.

AgNP-Coated Natural Compounds Showed Enhanced Antiamoebic Activity against *N. fowleri*. The amoebicidal assay was performed to examine the antiamoebic potential of AgNPs coated with natural compounds (AND-AgNPs, BOR-AgNPs, and FOR-AgNPs) against *N. fowleri* for the first time. The assay was performed in RPMI-1640 supplemented with penicillin–streptomycin (pen strip) to maintain the number of cells. The number of trophozoites in negative (trophozoites in RPMI-1640 supplemented with pen

strip only) and solvent control (water) were maintained at 2.7×10^5 and 2.5×10^5 cells/mL. The bar graph showed that all tested nanoconjugates significantly (*t*-test, *p* value < 0.05 with respect to vehicle control) reduced the viability of *N. fowleri* dose-dependently.

AND-AgNPs, BOR-AgNPs, and FOR-AgNPs significantly reduced the viability at 100 μ M from 3×10^5 to 1×10^5 (*p* = 0.04), 8.2×10^4 (*p* = 0.03), 7.3×10^4 (*p* = 0.02) cells/mL, as depicted in Figure 4A. Upon exposure to the highest concentration (75 μ M), AND-AgNPs, BOR-AgNPs, and FOR-AgNPs demonstrated the capacity to noticeably impede the viability of trophozoites, exhibiting inhibition rates of approximately 63.17, 69.55, and 72.90%, respectively, in comparison to the negative control, as illustrated in Figure 4B. The most efficient activity was recorded for FOR-AgNPs showing an $IC_{50}/24$ h at 26.35 ± 8.3 μ M, followed by BOR-AgNPs showing an $IC_{50}/24$ h at 36.24 ± 3.08 μ M (Table 1).

AgNP-Coated Natural Compounds Showed Enhanced Anticystic Activity against *N. fowleri*. The cysticidal assay was performed to determine the potential of nanoconjugates (AND-AgNPs, BOR-AgNPs, and FOR-AgNPs) against the cystic form of *N. fowleri*. The presented data were recorded after 24 h of incubation of cysts with different concentrations (25, 50, and 75 μ g/mL) of the nanoconjugates to determine IC_{50} concentration. The histogram in Figure 5A showed that all nanoconjugates significantly (*p* value < 0.05 with respect to vehicle control) inhibit the viability of cysts dose-dependently. Cysts alone in RPMI-1640 were used as the negative control, where the number of cysts was maintained at 1×10^5 cells/mL. Maximum activity was documented for FOR-AgNPs, which reduced the number of cells to 4×10^4 (*p* = 0.04) cells/mL as compared to negative control. The least activity was recorded for AND-AgNPs, which reduced the number of cysts to 4.7×10^5 (*p* = 0.01) cells/mL.

At the highest treatment concentration, AND-AgNPs, BOR-AgNPs, and FOR-AgNPs exhibited the ability to inhibit cyst viability by approximately 56.30, 54.00, and 63.36%, respectively, when compared to the negative control (as depicted in Figure 5B). Additionally, it is noteworthy that the IC_{50} value recorded for FOR-AgNPs over a 24 h period was 40.9 ± 3.42 μ M (Table 2).

AgNP-Coated Natural Compounds Showed Moderate Toxicity against HaCaT Cells. The possible toxicity of nanoconjugates (AND-AgNPs, BOR-AgNPs, and FOR-AgNPs) was assessed against the HaCaT cell line. In vitro cytotoxicity was determined by using the LDH kit. The histogram in Figure 6 shows that nanoconjugates showed dose-dependent toxicity. All conjugates showed higher toxicity as compared to AgNPs alone. The increase in toxicity of nanoconjugates is due to their conjugation with AgNPs alone. We evidently found that, at the tested concentration of 75 μ M, AND-AgNPs and BOR-AgNPs exhibited moderate toxicity (less than 40%) as the toxicity was 38.6 and 32.4%, respectively. However, at 75 μ M, the toxicity for FOR-AgNPs was higher, as it showed 41.5% toxicity against the HaCaT cells. So, 25 and 50 μ M were proved to be safe concentrations for FOR-AgNPs.

AgNP-Coated with Natural Compounds Significantly Inhibit *N. fowleri*-Mediated Host Cell Toxicity. Amoebas have the ability to induce programmed cell death (PCD) in host cells. Cytopathogenicity experiment was accomplished to evaluate the potential of AgNPs coated with natural

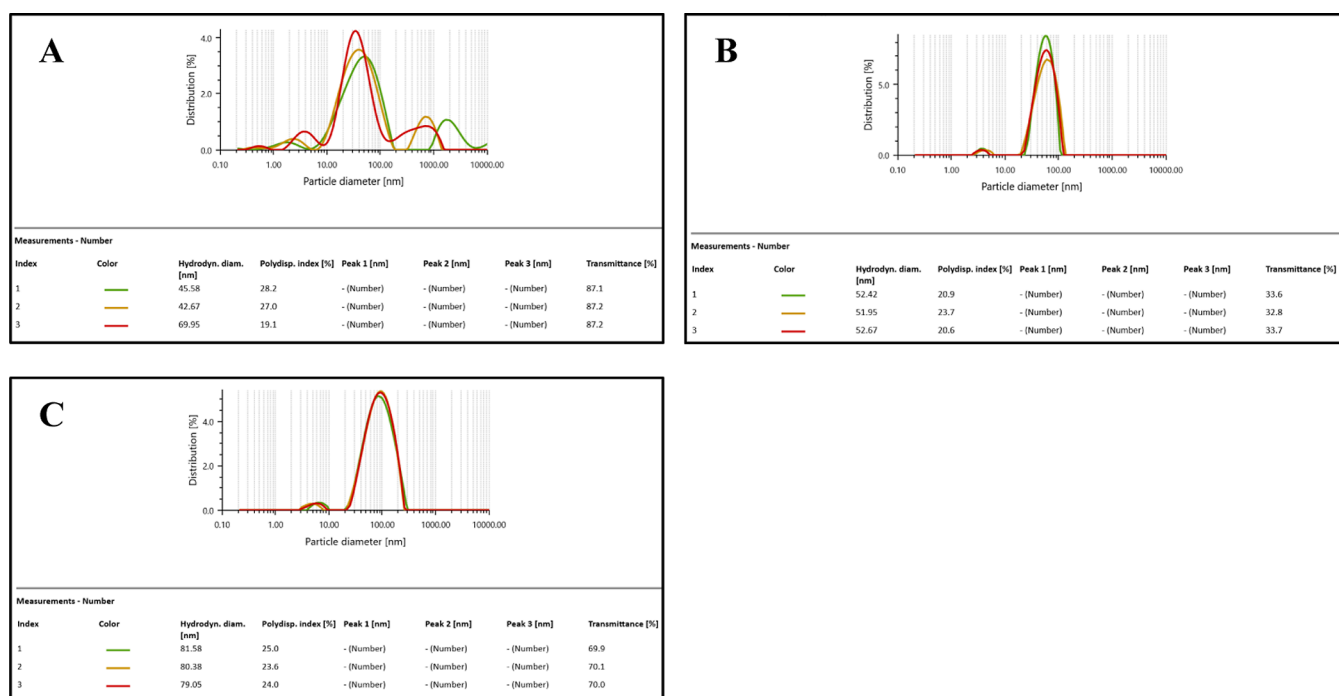


Figure 2. Particle size distribution of (A) AND-AgNPs, (B) BOR-AgNPs, and (C) FOR-AgNPs.

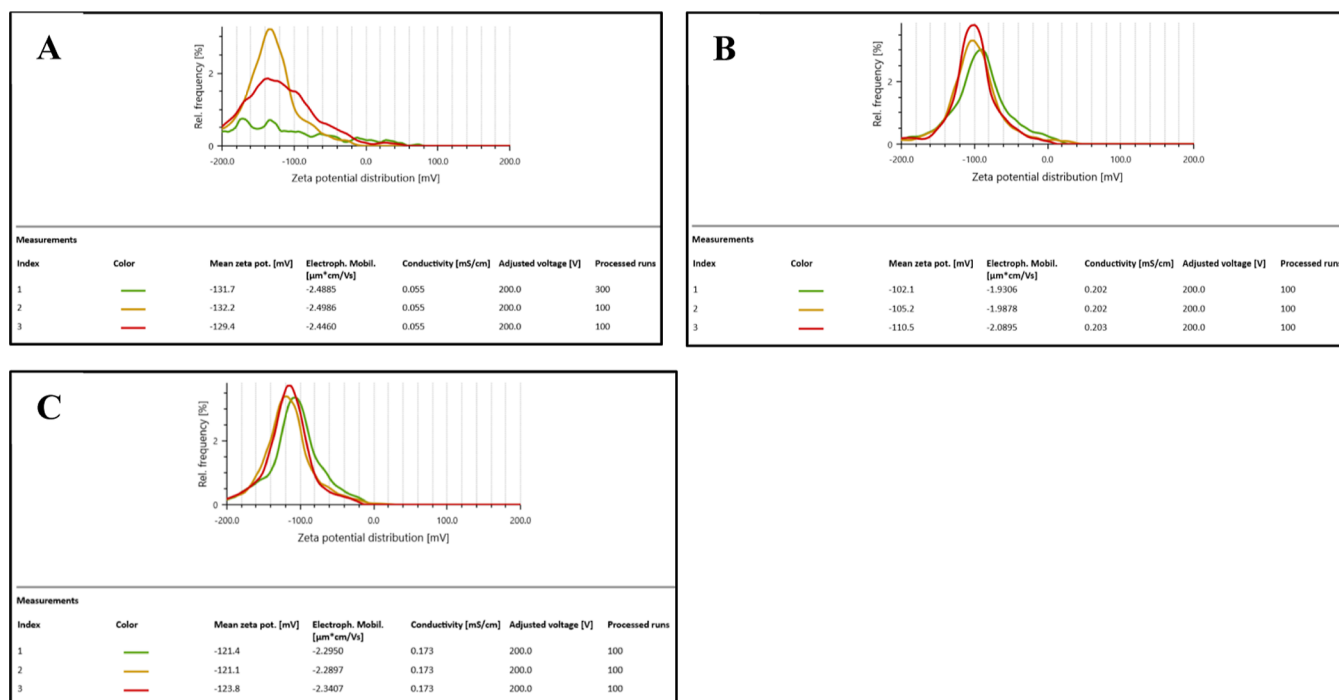


Figure 3. Size distribution of (A) AND-AgNPs, (B) BOR-AgNPs, and (C) FOR-AgNPs, confirming that nanoconjugates were highly stabilized during investigations.

compounds to prevent *N. fowleri*-mediated host cell toxicity. The trophozoites were pretreated with different concentrations of nanoconjugates (AND-AgNPs, BOR-AgNPs, and FOR-AgNPs) before challenging with HaCaT cells. The histogram of Figure 7 showed that all of the nanoconjugates inhibited cytopathogenicity dose-dependently. The HaCaT cells showed 73.3% sensitivity to untreated trophozoites. However, upon pretreatment with AND-AgNPs, BOR-AgNPs, and FOR-AgNPs, the cytopathogenicity significantly declined from 100

to 33.8, 26.4 and 28.03%, respectively. The maximum activity was recorded for BOR-AgNPs, followed by FOR-AgNPs and AND-AgNPs (Figure 7).

Discussion. Death rates associated with PAM stay relatively high despite the currently available treatments.¹ The known drug to treat PAM infections still faces obstacles in delivery due to its toxicity against human cells and poor BBB penetration.³⁶ Therefore, various compounds ranging from synthetic to natural have been tested against *N. fowleri*

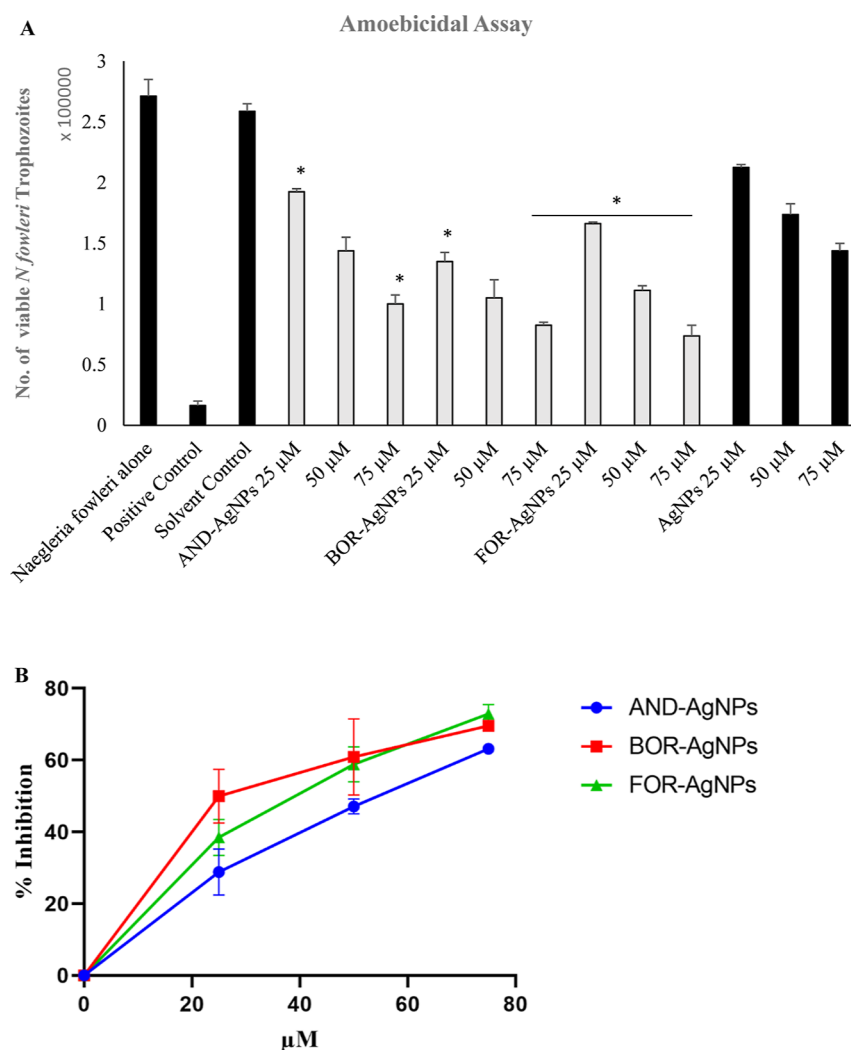


Figure 4. (A) Bar graph illustrates the antiamoebic potential of silver nanoconjugates, showing the viability of amoebic trophozoites compared to controls. Briefly, trophozoites of *N. fowleri* were subjected to a 24 h treatment with different concentrations (25, 50, and 75 μ M) of AgNPs coated with terpenes at 30 $^{\circ}$ C. Miltefosine (100 μ M) served as the positive control, water as the solvent control, and AgNPs alone (25, 50, and 75 μ M) acted as the vehicle control. “*” indicates a p value < 0.05 with respect to vehicle control. (B) Graphing the percentage of inhibition exhibited by nanoconjugates against the trophozoite stage of *N. fowleri* provides a visual representation of the inhibitory efficacy of these formulations.

Table 1. Comprehensive Overview of the Nanoconjugates Alongside Their Respective 50% Inhibitory Concentration (IC_{50}) Values against Trophozoites of *N. fowleri*

nanoconjugates	IC_{50} value (μ M)
AND-AgNPs	55.18 \pm 4.81
BOR-AgNPs	36.24 \pm 3.08
FOR-AgNPs	26.35 \pm 8.39

infection. However, most of the compounds are inactive against the cyst stage, have high toxicity, and are unable to cross BBB.^{28,32,37,38}

Nanotechnology holds the potential of transforming the landscape of diagnosis and therapy for human diseases. The unique capabilities of nanoscale materials offer innovative avenues for improving the precision and effectiveness of both diagnosing and treating.³⁹ Nanoparticles have attracted substantial interest in the medical field due to their unique characteristics and potential roles in addressing diverse human diseases.^{22,30} It has not only achieved significant success in the realm of cancer treatment but has also undergone extensive

investigation as an effective agent in combating infectious diseases.^{40,41} Nanoparticle drug delivery systems offer numerous advantages, primarily stemming from their diminutive size, which results in an increased surface area for absorption. They can be engineered by encapsulating specific drugs or compounds, and hence, can be delivered to target a specific cells.^{39,41} Beyond this, they enhance the stability as well as the solubility of partially water-soluble drugs or compounds and hence increase their bioavailability.⁴² Nanoparticles also enhance the ability of compounds to cross BBB⁴³ and target specific cells or tissues. They also assimilate therapeutic as well as diagnostic functions for immediate treatment and monitoring.⁴⁴ They have been proven to mitigate the toxicity of therapeutic drugs or compounds. Additionally, the controlled drug release feature of nanoparticle systems ensures that therapeutic agents are dispensed gradually and consistently, optimizing their efficacy while minimizing potential side effects.⁴⁵ These attributes make nanoparticle-based drug delivery systems an attractive option in the realm of pharmaceuticals.

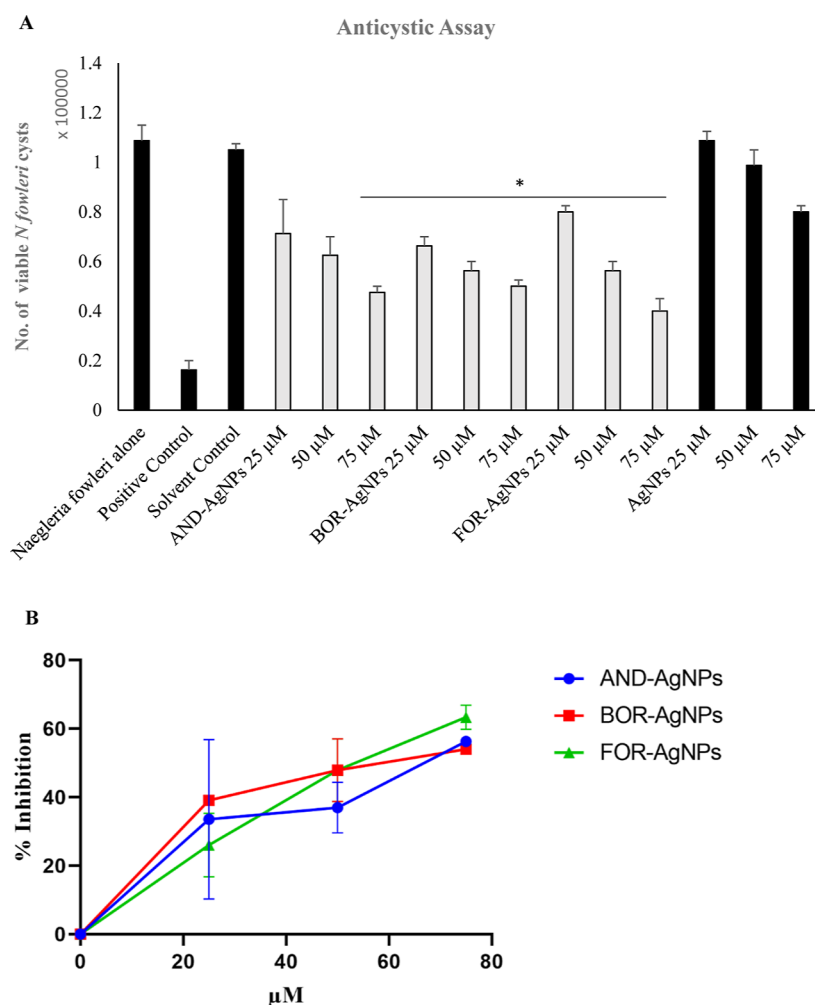


Figure 5. Anticystic assays: (A) bar graph illustrates the anticystic potential of silver nanoconjugates, showing the viability of *N. fowleri* cysts compared to controls. Briefly, 1×10^5 cysts were treated with different concentrations (25, 50, and 75 μM) of nanoconjugates for 24 h at 30 °C. Miltefosine (100 μM) served as the positive control, water as the solvent control, and AgNPs alone (25, 50, and 75 μM) acted as the vehicle control. “*” indicates a p value < 0.05. (B) Graphing the percentage of inhibition exhibited by nanoconjugates against the cyst stage of *N. fowleri* provides a visual representation of the inhibitory efficacy of these formulations.

Table 2. Comprehensive Overview of the Nanoconjugates Alongside Their Respective 50% Inhibitory Concentration (IC_{50}) Values against Cysts of *N. fowleri*

nanoconjugates	IC_{50} value (μM)
AND-AgNPs	43.99 ± 26.86
BOR-AgNPs	64.59 ± 7.94
FOR-AgNPs	40.90 ± 3.42

In recent years nanotechnology has gained more attention and researched extensively as an antimicrobial agent against infectious diseases.⁴⁵ Our group has previously conjugated the repurposed drugs with nanoparticles and tested against *N. fowleri*. The nanoconjugates showed higher antiameobic activity as compared to positive control.³² Similarly, AmpB and nystatin, two drugs widely used to treat PAM infections were conjugated with AgNPs, and the nanoconjugates displayed enhanced effects compared to the drugs alone.^{18,46} It is imperative to develop drugs that can successfully cross the BBB to target the infection sites of *N. fowleri* without inducing toxicity to the host’s cells while also reducing the progress of the infection.

In previous laboratory experiments, our research team conducted testing on FOR, AND, THY, and BOR within the context of a different pathogenic genus of free-living amoebae (FLA). The results of our investigations revealed that these compounds exhibited remarkable capability to effectively eradicate both life cycle stages of amoeba.⁴⁷ These findings are significant not only in terms of advancing our understanding of the potential applications of FOR, AND, THY, and BOR in combating parasitic infections but also in highlighting the broad spectrum of activity these compounds may possess against various amoebic pathogens. The former promising evidence⁴⁷ emphasizes the need for further research into the therapeutic potential of these compounds. Therefore, FOR, AND, and BOR were successfully coated with AgNPs and tested for their ability to combat *N. fowleri* infections, possibly opening up new paths for the development of innovative treatments and interventions in this sector.

Here, the hit compounds, such as FOR, AND, and BOR-conjugated AgNPs (FOR-AgNPs, AND-AgNPs, and BOR-AgNPs) were assessed in vitro for their effect on trophozoite and cyst stage of *N. fowleri*. All of the nanoconjugates used in this study effectively inhibit the viability of *N. fowleri*. These

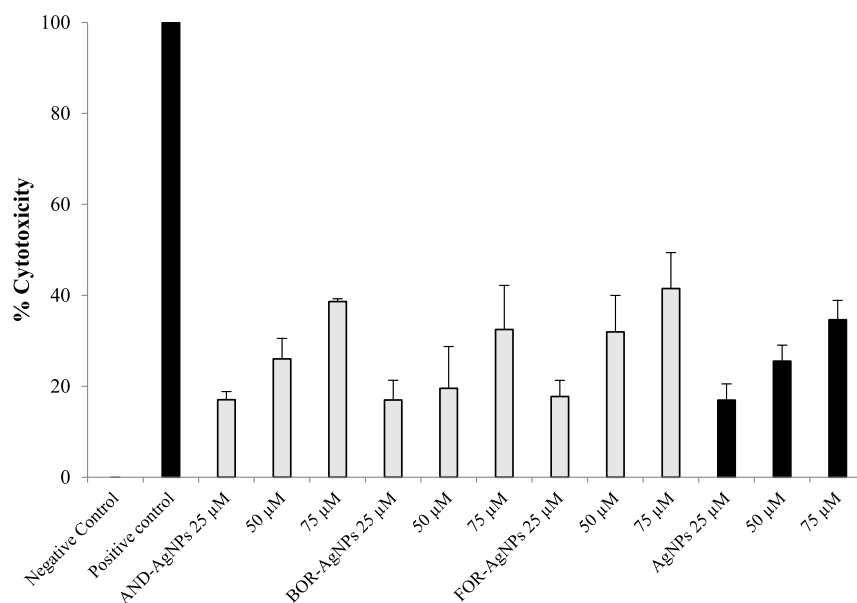


Figure 6. In vitro cytotoxicity assays: the histogram illustrates the toxic effect of silver nanoconjugates, showing the percentage of cytotoxicity compared to controls. The possible toxicity of nanoconjugates was assessed against a monolayer of the HaCaT cell line. The HaCaT cells were treated with different concentrations (25, 50, and 75 μM) of AgNPs coated with natural compounds for 24 h in a CO_2 incubator. 0.1% Triton X-100 served as the positive control, untreated HaCaT cells acted as a negative control, and AgNPs alone (25, 50, and 75 μM) acted as the vehicle control.

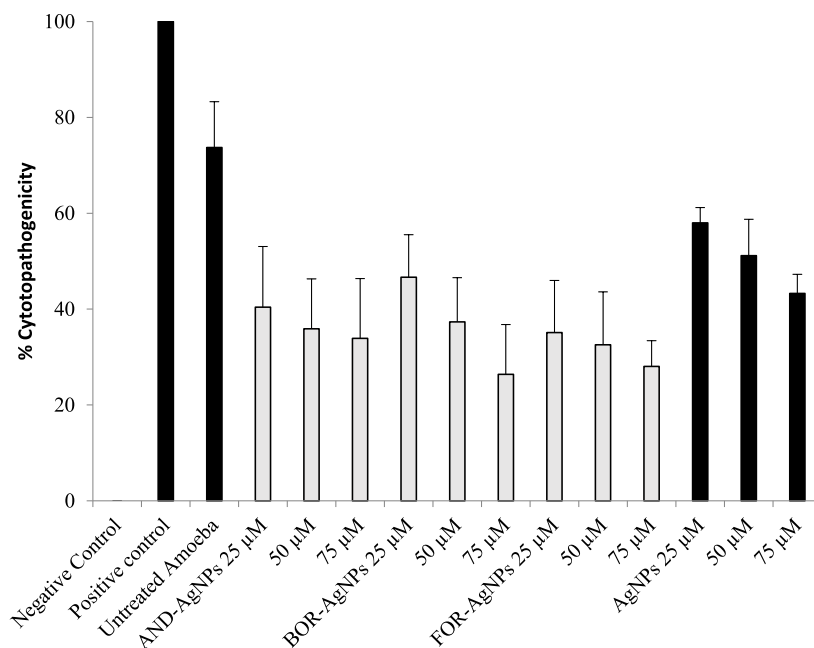


Figure 7. In vitro cytopathogenicity assays: the histogram illustrates the effect of silver nanoconjugates on the toxicity of *N. fowleri*, showing the percentage of cytopathogenicity as compared to controls. Briefly, the trophozoites were treated with different concentrations (25, 50, and 75 μM) of nanoconjugates for 2 h in a CO_2 incubator. After incubation, the HaCaT monolayer was treated with pretreated trophozoites overnight. 0.1% Triton X-100 served as the positive control, HaCaT cells treated with untreated trophozoites acted as untreated amoeba, and AgNPs alone (25, 50, and 75 μM) acted as the vehicle control. The experiment was performed thrice in duplicate.

nanoconjugates also showed minimal toxicity against the HaCaT cell line and effectively reduced the cytopathogenicity of *N. fowleri* trophozoites against human keratinocyte cells.

Furthermore, the amoebicidal assessment revealed that FOR-AgNPs, AND-AgNPs, and BOR-AgNPs exhibited significant antiamoebic activities against *N. fowleri*. These results showed that the antiamoebic potential of these nanoconjugates was higher than the previously calculated antiamoebic efficacy

of compounds alone.⁴⁷ Among the tested nanoconjugates, FOR-AgNPs showed the highest antiamoebic effects with an IC_{50} of 26.35 μM . These results were reinforced by Aykur et al.,²² where they conjugated the plant extract with different nanoparticles (silver, copper, and nickel) and assessed against FLA. The silver nanoconjugates showed enhanced antiamoebic activity as compared to other nanoconjugates.²² The anticystic assessment revealed that all nanoconjugates displayed

increased anticystic effects with the maximum activity recorded by FOR-AgNPs. These results emphasize the improved therapeutic promise of the nanoconjugates in combating amoebic infections, presenting a significant advancement in our understanding of their potential in the realm of amoebic pathogen control. Similarly, previous studies reported an increase in efficiency and a decrease in the minimum inhibitory concentration of drugs conjugated with nanoparticles.^{17,18} Our findings were corroborated by an additional investigation wherein oleic acid was conjugated with AgNPs, revealing enhanced amoebicidal effects against *N. fowleri* when compared to the conventional antiprotozoal agent AmpB alone.³² In another study, the coating of embelin with AgNPs demonstrated an improved anti-amoebic efficacy when contrasted with the use of the drugs alone, providing additional substantiation to our findings.²⁹ This highlights the potential synergistic effects of nanoconjugates, enhancing their therapeutic impact against amoebic infections.

The exact mechanism by which the tested nanoconjugates exert their effects on the trophozoite and cyst stages of *N. fowleri* remains elusive and is yet to be fully elucidated. However, an earlier investigation revealed that AND-AgNPs were evaluated against Gram-negative bacteria and exhibited robust antimicrobial activity. The observed antimicrobial effects were attributed to mechanisms such as the release of silver ions, generation of reactive oxygen species, alterations in membrane integrity and neutralization, etc.⁴⁸ BOR has undergone rigorous assessment in antimicrobial studies, wherein it has been shown to exert inhibitory effects on microbial adhesion to surfaces.⁴⁹ Recently, PCD has also been reported in FLA induced by nanoconjugates.²⁹ Similarly, sesquiterpenes lactones are also reported to cause PCD in *N. fowleri* trophozoites.⁵⁰ Furthermore, it has been documented that both AND BOR possess notable biological activity against pathogenic microorganisms.^{48,49} These delineated mechanisms represent the proposed mode of action caused by the tested nanoconjugates against *N. fowleri* and thus underscore the need for further scientific investigations to unravel the specific molecular and cellular processes involved in their action against this parasitic organism.

Upon establishing the robust activity of the nanoconjugates against both trophozoite and cyst stages of *N. fowleri*, we evaluated their cytotoxic effects on HaCaT cells. As we know, *N. fowleri* gains entry into the human body through the nasal mucosa, and the epithelial layer, primarily composed of keratinocytes, serves as the first line of defense against its invasion. Keratinocytes, which are key components of the epidermis, function as a vigorous barrier against external pathogens.^{1,47} In the present study, we employed HaCaT cells, renowned for its extensive use in examining epidermal homeostasis.^{1,51} The choice of HaCaT cells was driven by their facile replicability, maintaining an almost normal phenotype, serving as an effective keratinocyte model, and exhibiting characteristics conducive to the study of epidermal defense mechanisms. Additionally, their capacity to emulate barrier function against pathogens and drugs enhances their suitability for our research objectives. This step was pivotal in assessing the safety and selectivity of the nanoconjugates in a cellular context, as HaCaT cells serve as an established model for human keratinocytes.^{1,52} These cells have also been widely studied for nanoconjugate cytotoxicity and skin-related toxicity due to their retention of key characteristics.^{17,18,29,52} Their use is pivotal for assessing the safety of cosmetics, pharmaceuticals,

and topical products. This investigation aimed to determine the potential adverse effects of the tested nanoconjugates on these epidermal cells, which is a critical factor in assessing their therapeutic viability. Our study showed that AND-AgNPs and BOR-AgNPs revealed a toxicity of less than 40% at the highest tested concentration, while FOR-AgNPs showed a higher toxicity (41.5%) at 75 μM against the HaCaT cells. So up to 50 μM concentrations were proven to be safe for FOR-AgNPs. Host cell cytopathogenicity assays were also conducted against HaCaT cells. Our results are evident that untreated *N. fowleri* produced 73% cytopathogenicity to HaCaT cells while pretreatment with the nanoconjugates reduced the cytopathogenicity to below 60% with BOR-AgNPs having a decline to 26%. The scientific literature reports that AND-AgNPs were evaluated for their cytotoxicity against both Vero and MCF-7 breast cancer cell lines. The cells were exposed to up to 100 $\mu\text{g}/\text{mL}$ of nanoconjugate but demonstrated no cytotoxicity within 72 h of incubation,⁴⁸ which further confirms our results. Our results are also consistent with previous findings where drugs conjugated with AgNPs displayed enhanced anti-amoebic properties and moderate toxicity to HaCaT cells.^{18,32} A possible explanation could be that the AgNPs enhanced the transport of the natural compounds due to the decreased size of the nanoconjugates and increased surface area compared to those of the natural compounds alone.

The findings from this study contribute valuable insights into the biocompatibility and safety profile of the nanoconjugates, offering critical data for the development of a balanced therapeutic approach that effectively targets *N. fowleri* while minimizing harm to healthy human cells. These results represent a significant stride in the advancement of nano-therapeutics for protozoal infections and further reinforce the importance of judiciously considering the cytotoxicity profile in the development of novel antimicrobial agents. Further in-depth investigations, including the exploration of other cell lines (such as neuroblastoma) to assess possible toxicity, pharmacokinetics, and in vivo studies, are warranted to comprehensively assess the therapeutic potential of these nanoconjugates in clinical applications.

CONCLUSIONS

In the present study, a library of three natural compounds, such as AND, BOR, and FOR, were conjugated with AgNPs. These nanoconjugates were assessed against trophozoites and the cyst stage of *N. fowleri*. These nanoconjugates showed potent amoebicidal potential in vitro. Nanoconjugates have demonstrated a remarkable capacity to impede the phenotypic alteration of cysts, thereby showing their potent cysticidal properties. This, in turn, holds the potential to prevent the recurrence of infections. These nanoconjugates also effectively reduced the host cell toxicity caused by FLA while showing moderate toxicity to the HaCaT cell line, indicating a potential for enhancing the treatment of PAM infection. These findings imply that plant-based natural pharmacological entities should be further assessed in vitro and in vivo to be used as therapeutic agents to treat *N. fowleri* infections more effectively. Finally, these results not only show the efficacy of nanoconjugates but also expose new opportunities for the development of novel approaches to combat parasitic infections and reduce the risk of recurrence.

AUTHOR INFORMATION

Corresponding Authors

Kavitha Rajendran – School of American Education, Sunway University, Subang Jaya 47500 Selangor, Malaysia; orcid.org/0009-0008-1689-9387; Phone: 60-(0)3-7491-8622. Ext: 7207; Email: kavithar@sunway.edu.my

Ayaz Anwar – Department of Biological Sciences, School of Medical and Life Sciences, Sunway University, Subang Jaya 47500 Selangor, Malaysia; orcid.org/0000-0001-8638-3193; Phone: 60-(0)3-7491-8622. Ext: 7174; Email: ayazanwarkk@yahoo.com; Fax: 60-(0)3-5635-8630

Authors

Usman Ahmed – Department of Biological Sciences, School of Medical and Life Sciences, Sunway University, Subang Jaya 47500 Selangor, Malaysia

Alexia Chloe Meunier – Department of Biological Sciences, School of Medical and Life Sciences, Sunway University, Subang Jaya 47500 Selangor, Malaysia

Mohd Farooq Shaikh – Neuropharmacology Research Laboratory, Jeffrey Cheah School of Medicine and Health Sciences, Monash University Malaysia, Bandar Sunway 47500, Malaysia; School of Dentistry and Medical Sciences, Charles Sturt University, Orange 2800 New South Wales, Australia

Ruqaiyyah Siddiqui – Department of Microbiota Research Centre, Istinye University, Istanbul 34010, Turkey

Complete contact information is available at:

<https://pubs.acs.org/10.1021/acsomega.3c08844>

Author Contributions

K.R. and A.A. developed and supervised the study. K.R., U.A., and A.C.M. carried out the experiments against *N. fowleri* and compiled the first draft of the manuscript. M.F.S. carried out the analysis on the terpene compounds. A.A. and R.S. analyzed the data and finalized the manuscript submission. All authors contributed equally and approved the final manuscript.

Funding

This research work was supported by Sunway University, Malaysia [Internal grant scheme, GRTIN-KSGS(03)-CAE-02-2022].

Notes

The authors declare no competing financial interest.

ACKNOWLEDGMENTS

This research work was supported by Sunway University, Malaysia.

REFERENCES

- (1) Siddiqui, R.; Ali, I. K. M.; Cope, J. R.; Khan, N. A. Biology and pathogenesis of *Naegleria fowleri*. *Acta Trop.* **2016**, *164*, 375–394.
- (2) Visvesvara, G. S.; Moura, H.; Schuster, F. L. Pathogenic and opportunistic free-living amoebae: *Acanthamoeba* spp., *Balamuthia mandrillaris*, *Naegleria fowleri*, and *Sappinia diploidea*. *FEMS Microbiol. Immunol.* **2007**, *50* (1), 1–26.
- (3) Yoder, J. S.; Straif-Bourgeois, S.; Roy, S. L.; Moore, T. A.; Visvesvara, G. S.; Ratard, R. C.; Hill, V. R.; Wilson, J. D.; Linscott, A. J.; Crager, R.; Kozak, N. A.; et al. Primary amoebic meningoencephalitis deaths associated with sinus irrigation using contaminated tap water. *Clin. Infect. Dis.* **2012**, *55* (9), e79–e85.
- (4) Dingle, A. D.; Fulton, C. Development of the flagellar apparatus of *Naegleria*. *J. Cell Biol.* **1966**, *31* (1), 43–54.
- (5) Stahl, L. M.; Olson, J. B. Environmental abiotic and biotic factors affecting the distribution and abundance of *Naegleria fowleri*. *FEMS Microbiol. Ecol.* **2020**, *97* (1), fiae238.
- (6) Siddiqui, R.; Khan, N. A. Primary amoebic meningoencephalitis caused by *Naegleria fowleri*: an old enemy presenting new challenges. *PLoS Neglected Trop. Dis.* **2014**, *8* (8), No. e3017.
- (7) Jahangeer, M.; Mahmood, Z.; Munir, N.; Waraich, U. E. A.; Tahir, I. M.; Akram, M.; Ali Shah, S. M.; Zulfqar, A.; Zainab, R. *Naegleria fowleri*: Sources of infection, pathophysiology, diagnosis, and management; a review. *Clin. Exp. Pharmacol. Physiol.* **2020**, *47* (2), 199–212.
- (8) Shakoor, S.; Beg, M. A.; Mahmood, S. F.; Bandea, R.; Sriram, R.; Noman, F.; Ali, F.; Visvesvara, G. S.; Zafar, A. Primary amoebic meningoencephalitis caused by *Naegleria fowleri*, Karachi, Pakistan. *Emerging Infect. Dis.* **2011**, *17* (2), 258–261.
- (9) Trabelsi, H.; Dendana, F.; Sellami, A.; Sellami, H.; Cheikhrouhou, F.; Neji, S.; Makni, F.; Ayadi, A. Pathogenic free-living amoebae: epidemiology and clinical review. *Pathol. Biol.* **2012**, *60* (6), 399–405.
- (10) Grace, E.; Asbill, S.; Virga, K. *Naegleria fowleri*: pathogenesis, diagnosis, and treatment options. *Antimicrob. Agents Chemother.* **2015**, *59* (11), 6677–6681.
- (11) Visvesvara, G. S. Infections with free-living amoebae. *Handb. Clin. Neurol.* **2013**, *114*, 153–168.
- (12) Stevens, A. R.; Shulman, S. T.; Lansen, T. A.; Cichon, M. J.; Willaert, E. Primary amoebic meningoencephalitis: a report of two cases and antibiotic and immunologic studies. *J. Infect. Dis.* **1981**, *143* (2), 193–199.
- (13) Dorlo, T. P.; Balasegaram, M.; Beijnen, J. H.; de Vries, P. J. Miltefosine: a review of its pharmacology and therapeutic efficacy in the treatment of leishmaniasis. *J. Antimicrob. Chemother.* **2012**, *67* (11), 2576–2597.
- (14) Zhang, P.; Li, Y.; Tang, W.; Zhao, J.; Jing, L.; McHugh, K. J. Theranostic nanoparticles with disease-specific administration strategies. *Nano Today* **2022**, *42*, 101335.
- (15) Gurunathan, S.; Kang, M. H.; Qasim, M.; Kim, J. H. Nanoparticle-mediated combination therapy: Two-in-one approach for cancer. *Int. J. Mol. Sci.* **2018**, *19* (10), 3264.
- (16) Rai, M.; Yadav, A.; Gade, A. Silver nanoparticles as a new generation of antimicrobials. *Biotechnol. Adv.* **2009**, *27* (1), 76–83.
- (17) Anwar, A.; Masri, A.; Rao, K.; Rajendran, K.; Khan, N. A.; Shah, M. R.; Siddiqui, R. Antimicrobial activities of green synthesized gums-stabilized nanoparticles loaded with flavonoids. *Sci. Rep.* **2019**, *9* (1), 3122.
- (18) Anwar, A.; Siddiqui, R.; Hussain, M. A.; Ahmed, D.; Shah, M. R.; Khan, N. A. Silver nanoparticle conjugation affects antiacanthamoebic activities of amphotericin B, nystatin, and fluconazole. *Parasitol. Res.* **2018**, *117*, 265–271.
- (19) Padzik, M.; Hendiger, E. B.; Chomicz, L.; Grodzik, M.; Szmiedt, M.; Grobelny, J.; Lorenzo-Morales, J. Tannic acid-modified silver nanoparticles as a novel therapeutic agent against *Acanthamoeba*. *Parasitol. Res.* **2018**, *117*, 3519–3525.
- (20) Mahboob, T.; Nawaz, M.; Tian-Chye, T.; Samudi, C.; Wiart, C.; Nissapatorn, V. Preparation of poly (dl-lactide-co-glycolide) nanoparticles encapsulated with periglucine A and betulinic acid for in vitro anti-*Acanthamoeba* and cytotoxicity activities. *Pathogens* **2018**, *7* (3), 62.
- (21) Anwar, A.; Siddiqui, R.; Shah, M. R.; Khan, N. A. Gold Nanoparticle-Conjugated Cinnamic Acid Exhibits Antiacanthamoebic and Antibacterial Properties. *Antimicrob. Agents Chemother.* **2018**, *62* (9), 1110–1128.
- (22) Aykur, M.; Göksen Tosun, N.; Kaplan, O.; Özgür, A. Efficacy of the green synthesized silver, copper, and nickel nanoparticles using *Allium tuncelianum* extract against *Acanthamoeba castellanii*. *J. Drug Delivery Sci. Technol.* **2023**, *89*, 105013.
- (23) Zhang, H.; Li, S.; Si, Y.; Xu, H. Andrographolide and its derivatives: Current achievements and future perspectives. *Eur. J. Med. Chem.* **2021**, *224*, 113710.

- (24) Sokolova, A. S.; Yarovaya, O. I.; Shtro, A. A.; Borisova, M. S.; Morozova, E. A.; Tolstikova, T. G.; Zarubaev, V. V.; Salakhutdinov, N. F. Synthesis and biological activity of heterocyclic borneol derivatives. *Chem. Heterocycl. Compd.* **2017**, *53*, 371–377.
- (25) Mastan, A.; Rane, D.; Dastager, S. G.; Vivek Babu, C. S. Plant probiotic bacterial endophyte, *Alcaligenes faecalis*, modulates plant growth and forskolin biosynthesis in *Coleus forskohlii*. *Probiotics Antimicrob.* **2020**, *12*, 481–493.
- (26) Patel, M. B. Forskolol: A successful therapeutic phytomolecule. *East Cent. Afr. J. Pharmaceut. Sci.* **2010**, *13* (1), 25–32.
- (27) Behnia, M.; Haghghi, A.; Komeylzadeh, H.; Tabaei, S. J.; Abadi, A. Inhibitory effects of Iranian *Thymus vulgaris* extracts on in vitro growth of *Entamoeba histolytica*. *Korean J. Parasitol.* **2008**, *46* (3), 153.
- (28) Ahmed, U.; Manzoor, M.; Qureshi, S.; Mazhar, M.; Fatima, A.; Aurangzeb, S.; Hamid, M.; Khan, K. M.; Khan, N. A.; Rashid, Y.; Anwar, A. Anti-amoebic effects of synthetic acridine-9 (10H)-one against brain-eating amoebae. *Acta Trop.* **2023a**, *239*, 106824.
- (29) Ahmed, U.; Sivasothy, Y.; Khan, K. M.; Khan, N. A.; Wahab, S. M. A.; Awang, K.; Othman, M. A.; Anwar, A. Malabaricones from the fruit of *Myristica cinnamomea* King as potential agents against *Acanthamoeba castellanii*. *Acta Trop.* **2023b**, *248*, 107033.
- (30) Ahmed, U.; Ong, S. K.; Khan, K. M.; Siddiqui, R.; Khan, N. A.; Shaikh, M. F.; Alawfi, B. S.; Anwar, A. Effect of embelin on inhibition of cell growth and induction of apoptosis in *Acanthamoeba castellanii*. *Arch. Microbiol.* **2023c**, *205* (12), 360.
- (31) Rajendran, K.; Anwar, A.; Khan, N. A.; Shah, M. R.; Siddiqui, R. trans-Cinnamic acid conjugated gold nanoparticles as potent therapeutics against brain-eating amoeba *Naegleria fowleri*. *ACS Chem. Neurosci.* **2019**, *10* (6), 2692–2696.
- (32) Rajendran, K.; Anwar, A.; Khan, N. A.; Aslam, Z.; Raza Shah, M.; Siddiqui, R. Oleic Acid Coated Silver Nanoparticles Showed Better *in Vitro* Amoebicidal Effects against *Naegleria fowleri* than Amphotericin B. *ACS Chem. Neurosci.* **2020**, *11* (16), 2431–2437.
- (33) Eugin Simon, S.; Ahmed, U.; Saad, S. M.; Anwar, A.; Khan, K. M.; Tan, E. W.; Tan, K. O. New synthetic phenylquinazoline derivatives induce apoptosis by targeting the pro-survival members of the BCL-2 family. *Bioorg. Med. Chem. Lett.* **2022**, *67*, 128731.
- (34) Ahmed, U.; Ho, K. Y.; Simon, S. E.; Saad, S. M.; Ong, S. K.; Anwar, A.; Tan, K. O.; Sridewi, N.; Khan, K. M.; Khan, N. A.; Anwar, A. Potential anti-acanthamoebic effects through inhibition of CYP51 by novel quinazolinones. *Acta Trop.* **2022**, *231*, 106440.
- (35) Ahmed, D.; Anwar, A.; Khan, A. K.; Ahmed, A.; Shah, M. R.; Khan, N. A. Size selectivity in antibiofilm activity of 3-(diphenylphosphino) propanoic acid coated gold nanomaterials against Gram-positive *Staphylococcus aureus* and *Streptococcus mutans*. *AMB Express* **2017**, *7*, 210.
- (36) Lorenzo-Morales, J.; Khan, N. A.; Walochnik, J. An update on *Acanthamoeba keratitis*: diagnosis, pathogenesis and treatment. *Parasite* **2015**, *22*, 10.
- (37) Rice, C. A.; Colon, B. L.; Alp, M.; Göker, H.; Boykin, D. W.; Kyle, D. E. Bis-Benzimidazole Hits against *Naegleria fowleri* Discovered with New High-Throughput Screens. *Antimicrob. Agents Chemother.* **2015**, *59* (4), 2037–2044.
- (38) Anwar, A.; Mungroo, M. R.; Khan, S.; Fatima, I.; Rafique, R.; Kanwal, Khan, K. M.; Siddiqui, R.; Khan, N. A. Novel azoles as antiparasitic remedies against brain-eating amoebae. *Antibiotics* **2020**, *9* (4), 188.
- (39) Peer, D.; Karp, J.; Hong, S.; Farokhzad, O. C.; Margalit, R.; Langer, R. Nanocarriers as an emerging platform for cancer therapy. *Nat. Nanotechnol.* **2007**, *2* (12), 751–760. (2007)
- (40) Couvreur, P.; Vauthier, C. Nanotechnology: intelligent design to treat complex disease. *Pharm. Res.* **2006**, *23*, 1417–1450.
- (41) Ahmed, U.; Ong, S. K.; Tan, K. O.; Khan, K. M.; Khan, N. A.; Siddiqui, R.; Alawfi, B. S.; Anwar, A. Alpha-Mangostin and its nano-conjugates induced programmed cell death in *Acanthamoeba castellanii* belonging to the T4 genotype. *Int. Microbiol.* **2023**, *26*, 1–19.
- (42) Date, A. A.; Hanes, J.; Ensign, L. M. Nanoparticles for oral delivery: Design, evaluation and state-of-the-art. *J. Controlled Release* **2016**, *240*, 504–526.
- (43) Wohlfart, S.; Gelperina, S.; Kreuter, J. Transport of drugs across the blood–brain barrier by nanoparticles. *J. Controlled Release* **2012**, *161* (2), 264–273.
- (44) Jokerst, J. V.; Thangaraj, M.; Kempen, P. J.; Sinclair, R.; Gambhir, S. S. Photoacoustic imaging of mesenchymal stem cells in living mice via silica-coated gold nanorods. *ACS Nano* **2012**, *6* (7), 5920–5930.
- (45) Couvreur, P.; Vauthier, C. Nanotechnology: Intelligent Design to Treat Complex Disease. *Pharm. Res.* **2006**, *23* (7), 1417–1450.
- (46) Rajendran, K.; Anwar, A.; Khan, N. A.; Siddiqui, R. Brain-Eating Amoebae: Silver Nanoparticle Conjugation Enhanced Efficacy of Anti-Amoebic Drugs against *Naegleria fowleri*. *ACS Chem. Neurosci.* **2017**, *8* (12), 2626–2630.
- (47) Rajendran, K.; Ahmed, U.; Meunier, A. C.; Shaikh, M. F.; Siddiqui, R.; Anwar, A. Natural Terpenes Inhibit the Cytopathogenicity of *Naegleria fowleri* Causing Primary Amoebic Meningoencephalitis in the Human Cell Line Model. *ACS Chem. Neurosci.* **2023**, *14*, 4105–4114.
- (48) Thammawithan, S.; Talodthaisong, C.; Srichaiyapol, O.; Patramanon, R.; Hutchison, J. A.; Kulchat, S. Andrographolide stabilized-silver nanoparticles overcome ceftazidime-resistant *Burkholderia pseudomallei*: study of antimicrobial activity and mode of action. *Sci. Rep.* **2022**, *12* (1), 10701.
- (49) Ma, R.; Lu, D.; Wang, J.; Xie, Q.; Guo, J. Comparison of pharmacological activity and safety of different stereochemical configurations of borneol: L-borneol, D-borneol, and synthetic borneol. *Biomed. Pharmacother.* **2023**, *164*, 114668.
- (50) Arberas-Jimenez, I.; Rizo-Liendo, A.; Nocchi, N.; Sifaoui, I.; Chao-Pellicer, J.; Souto, M. L.; Suárez-Gómez, B.; Díaz-Marrero, A. R.; Fernández, J. J.; Piñero, J. E.; Lorenzo-Morales, J. Sesquiterpene lactones as potential therapeutic agents against *Naegleria fowleri*. *Biomed. Pharmacother.* **2022**, *147*, 112694.
- (51) Seo, M. D.; Kang, T. J.; Lee, C. H.; Lee, A. Y.; Noh, M. HaCaT keratinocytes and primary epidermal keratinocytes have different transcriptional profiles of cornified envelope-associated genes to T helper cell cytokines. *Biomol. Ther.* **2012**, *20* (2), 171–176.
- (52) Ahmed, U.; Anwar, A.; Ong, S. K.; Anwar, A.; Khan, N. A. Applications of medicinal chemistry for drug discovery against *Acanthamoeba* infections. *Med. Res. Rev.* **2022**, *42* (1), 462–512.